Condensation of ^{3}He and Reentrant Superfluidity in Submonolayer ^{3}He-^{4}He Mixture Films on H_2

G. A. Csáthy, E. Kim, and M. H. W. Chan

Department of Physics, Pennsylvania State University, University Park, Pennsylvania 16802

(Received 13 September 2001; published 8 January 2002)

We have studied the effect of ^{3}He on the superfluid response of submonolayer ^{4}He films adsorbed on H_2. In a limited range of ^{4}He coverage, the introduction of ^{3}He brings forth sequentially the normal, superfluid, and the normal phase again. This novel behavior is very likely the consequence of the condensation of the ^{3}He atoms confined near the free surface of the superfluid ^{4}He film into a self-bound 2D liquid.

DOI: 10.1103/PhysRevLett.88.045301 PACS numbers: 67.70.+n, 64.70.Fx, 67.60.Fp

Submonolayer methane and other classical atoms and molecules adsorbed on graphite [1] exhibit liquid-vapor phase separation that terminates at a critical point. This transition is a physical realization of the celebrated 2D Ising model [2]. There is considerable interest [3] on whether physisorbed ^{4}He and particularly ^{3}He monolayer films also exhibit this transition, since large zero point energy combined with weak interatomic attraction tends to suppress the condensation of 2D self-bound liquid patches. 2D liquid-vapor phase separation, with a critical point at 0.9 K, is found for ^{4}He on H_2 plated graphite [4]. The dilution of ^{4}He with ^{3}He suppresses the critical temperature [5]. There were a number of experiments studying pure ^{3}He adsorbed on graphite and on graphite plated with H_2, HD, and ^{4}He [4,6]. The ^{3}He films on the preplated substrates and the film beyond the first solid layer on graphite behave as a uniform 2D Fermi fluid below 0.1 K, with no evidence of formation of self-bound liquid and, hence, no evidence of 2D liquid-vapor coexistence.

In contrast to H_2 plated graphite [4], on amorphous substrates such as glass [7], gold [8], and H_2 plated gold [8,9], the adsorbed ^{4}He films do not appear to separate into liquid and vapor phases. When the ^{4}He coverage exceeds the inert coverage n_0, superfluidity sets in at a temperature that varies smoothly with coverage [7–9]. Superfluid ^{4}He films provide a new environment for ^{3}He atoms [10–15]. At low temperatures, the difference in molar volumes of the isotopes causes a preferential adsorption of ^{4}He close to the substrate and confinement of ^{3}He near the surface of the film [10–13]. One of the most fascinating results in this system is that reported by Gasparini and collaborators [11] of ^{3}He on ^{4}He films with approximately one superfluid layer adsorbed onto Nuclepore. In the vicinity of 0.1 K, the heat capacity of this system shows a sharp change from being temperature independent to being linear with temperature. This result was interpreted [11] as evidence of the ^{3}He entering the coexistence region of 2D vapor and self-bound 2D Fermi liquid. The critical temperature was deduced to be about 0.1 K. Hallock and co-workers [12] have performed NMR, third sound, and heat capacity measurements of the system under similar conditions. However, they found no evidence of any 2D phase separation. They [12] and other investigators [14] found that the mobile ^{3}He in the presence of superfluid ^{4}He films behaves as a uniform Fermi fluid. Theoretical investigations found support for both the absence [16] and the possibility [17] of phase separation into self-bound liquid and vapor phases. In this Letter, we report a study of the ordering and superfluidity of ^{3}He-^{4}He mixture films adsorbed on H_2. Superfluidity is unexpectedly enhanced with the addition of ^{3}He for films with a superfluid ^{4}He coverage between 0.05 and 0.08 layers and ^{3}He coverage between 0.26 and 0.49 layers. The liquid monolayer coverages are 12.9 μmol/m^2 for ^{4}He and 10.6 μmol/m^2 for ^{3}He, respectively. We think this behavior is driven by the condensation of ^{3}He atoms into a 2D self-bound liquid.

The torsional oscillator cell with the porous gold sample is the same we used in a number of recent experiments [8,13]. The porous gold is made up of interconnected gold strands of 0.06 μm in diameter. In this experiment, the gold surface has been preplated with approximately four layers of H_2. Because of capillary condensation into the corners where the gold strands join, the surface area of the H_2 preplated cell is about 10% smaller than that without preplating. The surface area is calibrated by means of T_s, the superfluid onset temperature, versus n_4, the ^{4}He coverage [8].

For each of the 14 runs, n_4 is kept constant and ^{3}He is added incrementally to the mixture film. To obtain consistent results, it is necessary to anneal the films to about 1.3 K after each addition of ^{3}He and/or ^{4}He. By repeating the annealing procedure several times without adding new helium to the cell, T_s reproduces to within 0.5 mK. The superfluid response and T_s are not history dependent; the results found for a mixture film of specific ^{3}He and ^{4}He content are reproducible irrespective of the order of addition of the isotopic components.

The curve with the highest T_s at 0.53 K in the inset of Fig. 1 shows the superfluid response of a pure ^{4}He film with $n_4 = 12.27$ μmol/m^2 or a superfluid coverage of $n_{4s} = 6.17$ μmol/m^2. Here $n_{4s} = n_4 - n_0$. While on

 © 2002 The American Physical Society

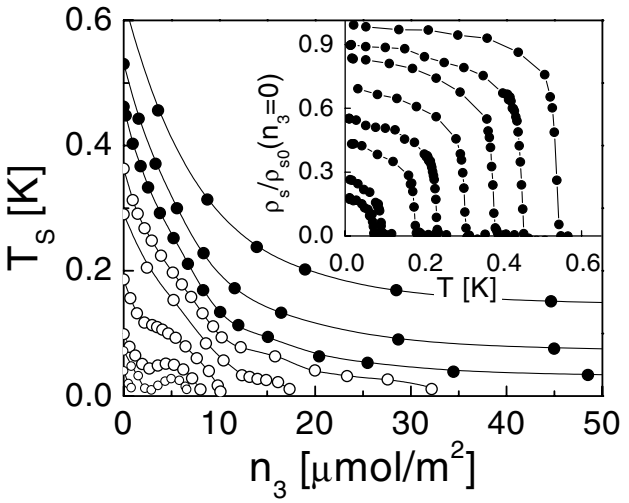

FIG. 1. Superfluid onset temperature T_s versus n_3 for nine mixture films of different n_4 on H_2. Values of n_4 are 6.73, 7.22, 7.60, 8.69, 9.79, 10.52, 11.56, 12.27, and 13.46 μmol/m^2. Lines are guides to the eye. The inset shows the evolution of the superfluid density ρ_s for the film with $n_4 = 12.27$ μmol/m^2 when 0, 1.57, 3.35, 5.57, 8.35, 11.60, 28.69, and 85.10 μmol/m^2 of ^{3}He is added to the film.

most substrates, such as gold [8], n_0 is on the order of two monolayers, on H_2 it is reduced to only 6.1 μmol/m^2 [8,9]. T_s can be determined by either extrapolating the superfluid density to zero or by locating the maximum of the dissipation peak that accompanies the onset of superfluidity. The two values are always within 6% of each other when $T_s > 30$ mK. For $T_s < 15$ mK we use the dissipation peak, since we cannot extract T_s reliably from the superfluid density data.

The inset of Fig. 1 shows that T_s is suppressed with the addition of ^{3}He, a result consistent with early findings [15]. We can understand this phenomenologically as a consequence of the entrainment of the superfluid into a normal fraction in the immediate vicinity of ^{3}He atoms, forming a halo of normal fluid around them. In Fig. 1 we summarize the evolution of T_s with n_3 for several films. Although the initial addition of ^{3}He causes a rapid suppression of T_s, this suppression decelerates exponentially with further enrichment of ^{3}He. Superfluidity persists in films with $n_4 > n_4^{\rm crit} = 11.1$ μmole/m^2, even in the presence of a very thick ^{3}He layer. These curves are marked by filled symbols. On the other hand, films with $n_4 < n_4^{\rm crit}$ marked with open symbols in Fig. 1 have a vanishing T_s at a well determined n_3.

The most striking feature of Fig. 1 is the undulating T_s dependence on n_3 for curves with low n_4. This is shown in more detail in Fig. 2a. For example, for the film with $n_4 = 7.60$ μmol/m^2, after an initial suppression, T_s is enhanced with increasing n_3. Further addition of ^{3}He then causes T_s to vanish. ρ_{s0}, the zero temperature superfluid density, has a similar behavior. This is the case, as shown in Fig. 3, even in the region where T_s increases with n_3.

The dependence of T_s on both n_3 and n_4 is shown in Fig. 4. This phase diagram is obtained by interpolating

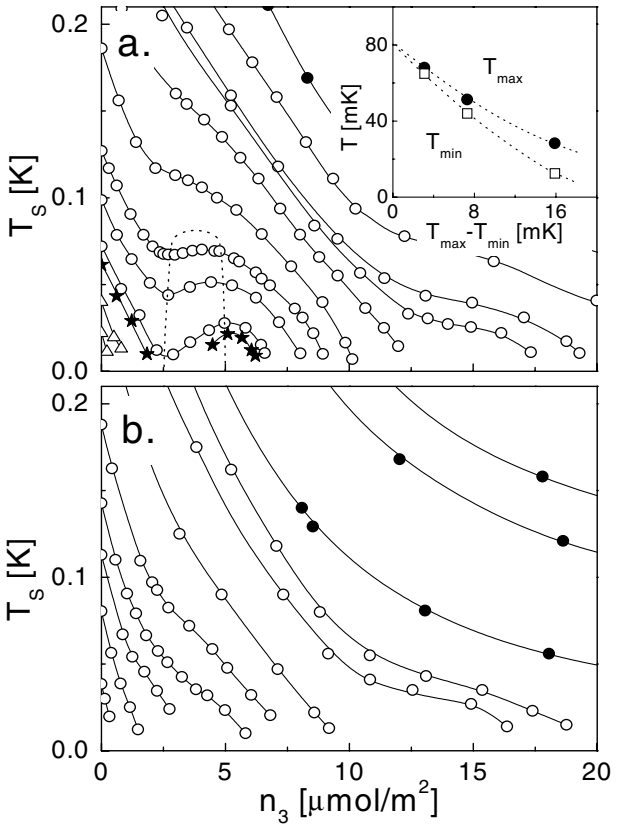

FIG. 2. Detailed view of the dependence of T_s on n_3 for films on H_2 [panel (a)] and Au [panel (b)] for ^{3}He coverages up to two monolayers. The ^{4}He coverages are 6.39, 6.73, 7.06, 7.22, 7.60, 7.97, 8.69, 9.37, 9.79, 9.93, 10.52, and 11.56 μmol/m^2 on H_2 and 25.80, 26.42, 26.87, 27.27, 27.80, 28.60, 29.35, 30.04, 30.70, 32.33, and 33.39 μmol/m^2 on Au, respectively. Inset of Fig. 2a shows how the liquid-vapor critical temperature is determined.

the T_s versus n_3 results. The 3D phase sheet of Fig. 4 separates the normal (above) and the superfluid (below) phases, and the undulating dependence of T_s on n_3 appears as a valley. The $T = 0$ phase boundary in the n_3-n_4 plane, shown as a red line in Fig. 4 and quantitatively

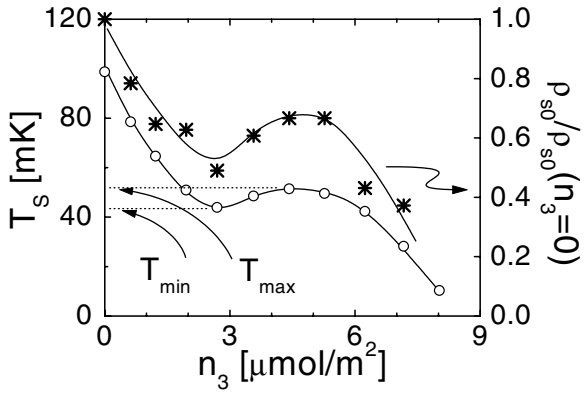

FIG. 3. The dependence of T_s and ρ_{s0} for films with $n_4 = 7.60$ μmol/m^2. $T_{\rm min}$ and $T_{\rm max}$, used in the inset of Fig. 2a, are also shown. The n_3 values at $T_{\rm min}$ and $T_{\rm max}$ define the extent of the coexistence region.

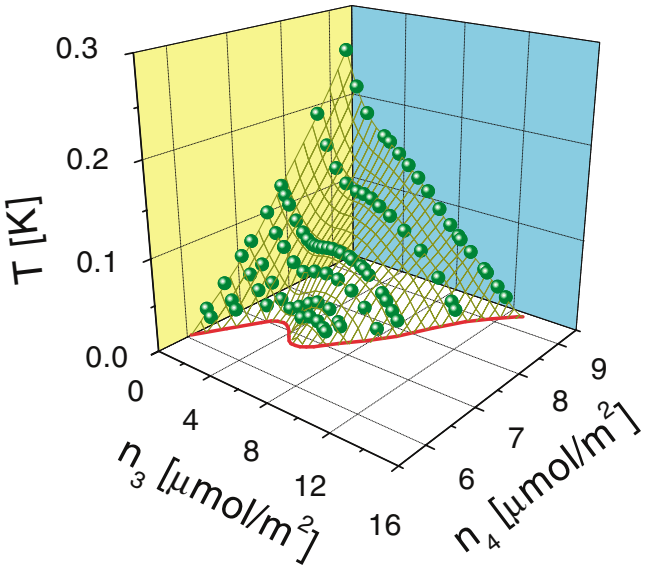

FIG. 4 (color). The phase diagram at low n_3 of ^{3}He-^{4}He mixture films adsorbed on H_2. The onset sheet separates the superfluid (below) and the insulating (above) regions. Eight data sets, with n_4 of 6.39, 6.73, 7.06, 7.22, 7.60, 7.97, 8.69, and 9.37 μmol/m^2, are marked by solid spheres. The thick red line is the $T = 0$ phase boundary.

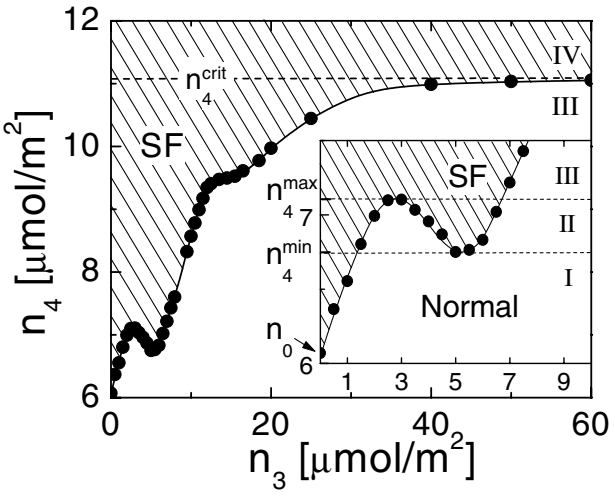

FIG. 5. The $T = 0$ phase diagram. The inset shows details at low n_3 and n_4. See text for descriptions of the different regions separated by n_0, n_4^{min}, n_4^{max}, and n_4^{crit}.

displayed in Fig. 5, is deduced by linearly extrapolating the lowest measured T_s at specific n_3 and n_4 values. This phase boundary originates from $n_4 = n_0$ at $n_3 = 0$. With increasing n_3, it develops a local maximum at $n_3 = 2.8$ μmol/m^2 or 0.26 layers, followed by a local minimum at $n_3 = 5.2$ μmol/m^2 or 0.49 layers, as shown in Fig. 5. The ^{4}He coverages of the local maximum and minimum are $n_4^{min} = 6.75$ and $n_4^{max} = 7.10$ μmol/m^2, respectively. At large n_3, this curve tends to n_4^{crit} asymptotically.

The $T = 0$ phase boundary allows us to classify the different T_s versus n_3 dependences shown in Figs. 1 and 2a. For films with $n_0 < n_4 < n_4^{min}$ (region I in Fig. 5), T_s decreases monotonically and vanishes with n_3. Examples are the two curves with the lowest T_s shown in open triangles in Fig. 2a. As noted earlier, for $n_4 > n_4^{crit}$ (region IV) superfluidity persists irrespective of how much ^{3}He is added to the film. Mixture films with n_4 on the order and larger than n_4^{max} (region III) show undulating T_s and ρ_{s0} as a function of n_3. As n_4 is increased farther from n_4^{max}, the undulation smoothes into a dependence with an inflection point and then exponentially decreases with n_3. The most interesting is region II, for which n_4 lies between n_4^{min} and n_4^{max}. Here, even in the $T = 0$ limit, the addition of ^{3}He first completely destroys superfluidity. With further addition of ^{3}He, superfluidity reappears before it is suppressed again. The curve marked by dark stars in Fig. 2a appears to follow this sequence of phase transitions.

ρ_{s0} can be enhanced only if the addition of ^{3}He releases some of the previously entrained, localized ^{4}He atoms into the superfluid film. A possible source of normal ^{4}He is the inert layer localized by the H_2 substrate. Because of the different zero point energies of ^{3}He and ^{4}He, the difference in the adsorption energy is estimated to be of the order of 2 K [18], more than 1 order of magnitude larger than 0.08 K, the highest temperature at which the undulation in T_s and ρ_{s0} is found. Therefore, the replacement of ^{4}He atoms from the inert layer by ^{3}He is very unlikely to occur. Nevertheless, we have tested for this possibility by not annealing when introducing 0.14 and 0.25 layers of ^{3}He into the cell prior to introducing ^{4}He. In both cases, the measured inert ^{4}He, determined by measuring T_s against subsequent addition of ^{4}He, is always larger than n_0, indicating that ^{3}He cannot be coaxed to replace ^{4}He from the inert layer.

The most likely source of ^{4}He that enhances superfluidity is the normal fluid entrained by ^{3}He atoms floating on the superfluid film. This normal fluid is released as a consequence of condensation of ^{3}He into a 2D liquid. The suppression of the superfluid response at dilute ^{3}He concentrations, i.e., $n_3 < 0.26$ layers, reflects the increase of the number of ^{3}He impurities and the normal ^{4}He halos surrounding them. For these coverages, ^{3}He forms a 2D gas. Beyond this value, the interaction among the ^{3}He atoms, possibly mediated by the superfluid film, induces the clustering of the gaslike atoms into 2D liquid patches. As a result, the individual halos also coalesce, hence, reducing the total area of contact between the ^{3}He atoms and the superfluid film and reducing the normal fluid fraction entrained. Four mixture films with n_4 between 7.06 and 7.97 μmol/m^2, shown in Fig. 2a, exhibit enhancement of the superfluid response with the addition of ^{3}He. Condensation into 2D liquid patches begins to take place when n_3 exceeds 2.8 μmol/m^2 and completes near $n_3 = 5.2$ μmol/m^2. It is quite remarkable that these n_3 values are quite insensitive to n_4. Beyond 5.2 μmol/m^2, the addition of ^{3}He serves to increase the areal density of the uniform 2D ^{3}He liquid. Figure 2a also shows that the undulation in T_s smoothes to be inflection pointlike

for the film with $n_4 = 8.69\ \mu\text{mol/m}^2$ and disappears for films with even higher n_4. These results suggest the presence of a 2D ^{3}He liquid-vapor coexistence region, with its boundary shown in dotted lines in Fig. 2a. While the shape of the coexistence boundary below 0.07 K is clearly defined by the local minima and maxima of T_s versus n_3 curves, above 0.07 K is less certain. We estimate the critical temperature by first identifying the temperatures of the local minimum (T_{min}) and maximum (T_{max}) from the three curves of Fig. 2a exhibiting both features and then plotting T_{min} and T_{max} as a function of their difference $T_{\text{max}} - T_{\text{min}}$. The critical temperature is given by the condition $T_{\text{max}} - T_{\text{min}} = 0$. The extrapolation, shown in the inset of Fig. 2a, yields a critical temperature of 0.080 ± 0.007 K.

Curves of Fig. 2a show a second inflection near $T = 0.02$ K and $n_3 = 14\ \mu\text{mol/m}^2$. Since this coverage exceeds the monolayer coverage, the inflection feature suggests the presence of another liquid-vapor coexistence of ^{3}He that lies on top of the first completed ^{3}He layer, with a critical temperature below 0.02 K. It is interesting to note that such a feature with nearly identical temperature and n_3 value is also present for mixture films adsorbed onto a gold surface without H_2 preplating (see Fig. 2b). This is the case even though there is no evidence of coexistence at submonolayer ^{3}He coverages on Au. We do not know why liquid-vapor separation for the first ^{3}He layer exists only on the H_2 preplated surface.

In conclusion, superfluid measurements reveal the presence of 2D liquid-vapor coexistence of ^{3}He near the free surface of a very thin superfluid ^{4}He film. The critical temperature of 0.08 K, similar to that of Ref. [11], is the lowest observed for a liquid-vapor transition. Our results for the second layer of ^{3}He indicate the possibility of an even lower critical point near or below 0.02 K. In contrast to the result of Gasparini [11], we find that the areal density of gas at which liquid condensation occurs is not negligible, but is 0.26 of a full liquid layer. The Fermi temperature of the gas prior to condensation, calculated with an effective mass that is 1.73 times the bare value [11], exceeds the critical temperature by a factor of 6. Therefore, a high precision heat capacity measurement of this system from the very dilute ^{3}He limit to the condensation density should show an evolution from 2D classical to quantum gas behavior. Extending the measurements to higher densities will allow the mapping of the 2D Fermi gas–Fermi liquid boundary near the critical point and reveal whether this transition also belongs to the 2D Ising universality class.

We thank M. W. Cole, F. M Gasparini, R. B. Hallock, and O. E. Vilches for stimulating discussions, and J. Yoon and D. J. Tulimieri for assistance in the early stages of the experiment. This work was supported by NSF DMR-9971471.

[1] H. K. Kim and M. H. W. Chan, Phys. Rev. Lett. **53**, 170 (1984); M. H. W. Chan, in *Phase Transitions in Surface Films, II,* edited by H. Taub, G. Torzo, H. J. Lauter, and S. Fain, Jr. (Plenum, New York, 1991), p. 1.
[2] L. Onsager, Phys. Rev. **65**, 117 (1944); C. N. Yang, Phys. Rev. **85**, 808 (1952).
[3] M. D. Miller and L. H. Nosanow, J. Low Temp. Phys. **32**, 145 (1978); E. Cheng *et al.,* Physica (Amsterdam) **177A**, 466 (1991); B. Brami *et al.,* J. Low Temp. Phys. **94**, 63 (1994).
[4] R. C. Ramos *et al.,* J. Low Temp. Phys. **110**, 615 (1998).
[5] R. C. Ramos and O. E. Vilches, J. Low Temp. Phys. **113**, 981 (1998).
[6] S. W. Van Sciver and O. E. Vilches, Phys. Rev. B **18**, 285 (1978); D. S. Greywall, Phys. Rev. B **41**, 1842 (1990); K.-D. Morhard, J. Low Temp. Phys. **101**, 161 (1995); M. Morishita *et al.,* J. Low Temp. Phys. **110**, 351 (1998); C. P. Lusher *et al.,* Phys. Rev. Lett. **67**, 2497 (1991); A. Casey *et al.,* J. Low Temp. Phys. **113**, 293 (1998).
[7] P. A. Crowell *et al.,* Phys. Rev. B **55**, 12 620 (1997).
[8] G. A. Csáthy *et al.,* Phys. Rev. Lett. **80**, 4482 (1998); G. A. Csáthy and M. H. W. Chan, J. Low Temp. Phys. **121**, 451 (2000).
[9] P. S. Ebey *et al.,* J. Low Temp. Phys. **110**, 635 (1998).
[10] M. J. DiPirro and F. M. Gasparini, Phys. Rev. Lett. **44**, 269 (1980); F. M. Ellis *et al.,* Phys. Rev. Lett. **46**, 1461 (1981); D. McQueeney *et al.,* Phys. Rev. Lett. **52**, 1325 (1984); J. P. Romagnan *et al.,* Phys. Rev. B **37**, 5639 (1988).
[11] B. Bhattacharyya and F. M. Gasparini, Phys. Rev. Lett. **49**, 919 (1982); B. K. Bhattacharyya and F. M. Gasparini, Phys. Rev. **B31**, 2719 (1985).
[12] F. M. Ellis and R. B. Hallock, Phys. Rev. B **29**, 497 (1984); J. M. Valles, Jr. *et al.,* Phys. Rev. Lett. **60**, 428 (1988); R. H. Higley *et al.,* Phys. Rev. Lett. **63**, 2570 (1989); N. Alikacem *et al.,* Phys. Rev. Lett. **67**, 2501 (1991); P.-C. Ho and R. B. Hallock, Phys. Rev. Lett. **87**, 135301 (2001).
[13] G. A. Csáthy and M. H. W. Chan, Phys. Rev. Lett. **87**, 045301 (2001).
[14] M. Dann *et al.,* Phys. Rev. Lett. **82**, 4030 (1999); N. Wada *et al.,* J. Low Temp. Phys. **113**, 317 (1998).
[15] E. N. Smith *et al.,* J. Phys. (Paris), Colloq. **39**, C6-342 (1978); E. Webster *et al.,* Phys. Rev. Lett. **42**, 243 (1979); J. P. Laheurte *et al.,* Phys. Rev. B **22**, 4307 (1980).
[16] R. H. Anderson and M. D. Miller, Phys. Rev. B **48**, 10 426 (1993).
[17] R. A. Guyer, Phys. Rev. Lett. **53**, 795 (1984).
[18] F. London, in *Superfluids* (Dover, New York, 1964), Vol. 2, p. 30.